iScience, Volume *24*

Supplemental information

Inter-organelle interactions between the ER and mitotic spindle facilitates Zika protease cleavage of human Kinesin-5 and results in mitotic defects

Liqiong Liu, Micquel Downs, Jesse Guidry, and Edward J. Wojcik

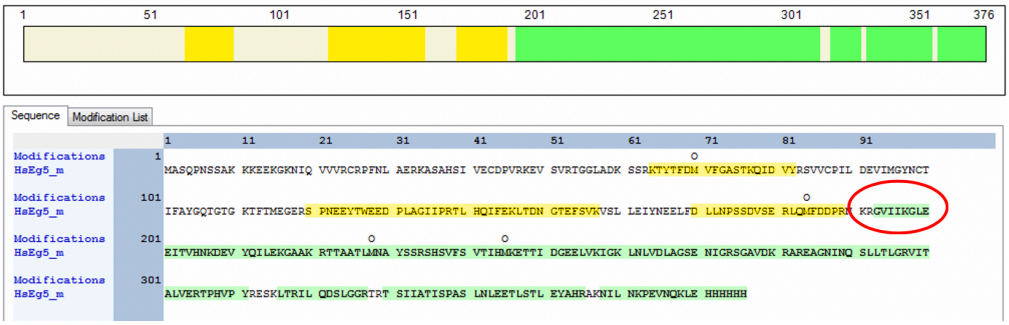

Figure S1. Peptide coverage map by LC-MS of the C-terminal product of *in vitro* digestion of HsEg5 motor domain by soluble ZPrC, related to Table 1 (asterisk). This data confirms cleavage of HsEg5 motor domain by ZPrC at the sequence $_{187}$DPRNKR^G$_{193}$ of loop8. The 20.4 kDa fragment of HsEg5 was excised (Figure 1) and processed for LC-MS. Greater than 97% of the trypsinized Peptide Spectral Matches (PSMs) map to peptides corresponding to the 20.4 kDa C-terminal segment of the HsEg5 motor domain (shaded green) that was predicted by the cleavage consensus (Table 1). Three peptides from the N-terminus upstream of residue 197 (shaded yellow) were also detected but represent less than 3% of the total PSMs. The N-terminus of the excised peptide begins from the ZPrC cleavage-site glycine (circled, red).

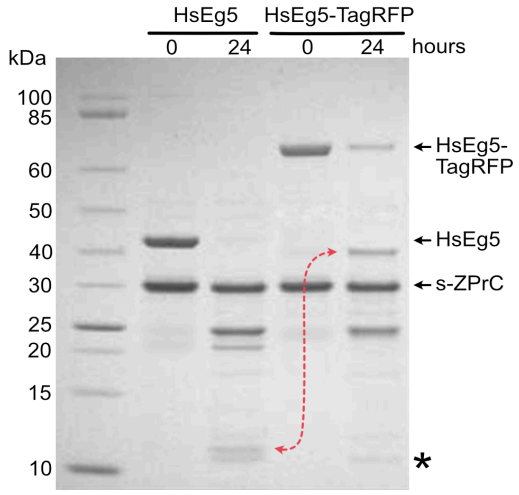

Figure S2. ***In vitro*** **digestion of HsEg5 motor domain with C-terminal TagRFP by s-ZPrC chimera identifies the C-terminal-most cleavage site at** $_{276}$**GAVDKR^A**$_{282}$**, related to Figure 1.** The primary cleavage site in the motor domain, $_{187}$DPNKR^G$_{193}$, is nearly completely cleaved in HsEg5 and moderately cleaved in HsEg5-TagRFP. The HsEg5 C-terminal 10.5 kDa fragment (red arrow) is upshifted to 40.5 kDa with the added TagRFP (30 kDa), while leaving the 9.5 kDa fragment as it was (asterisk).

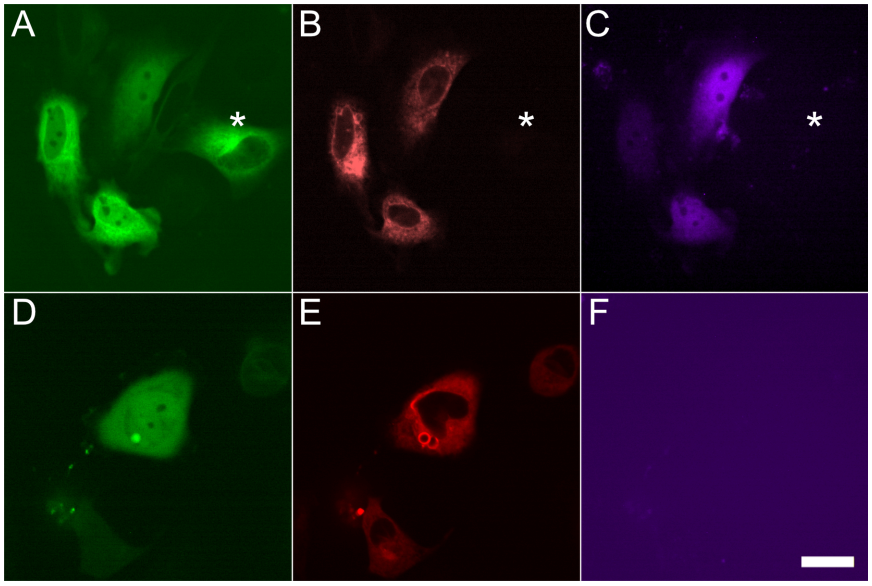

Figure S3. Live-cell imaging of Tub-GFP HeLa cells co-expressing ER-localized sZPrC-TagRFP-ER can hydrolyze the soluble HsEg5 biosensor mimic, related to Figure 9. Cells expressing the HsEg5 biosensor (A, green) display nucleocytoplasmic localization of the reporter in contrast to the microtubule network highlighted by tubulin-eGFP. Cells expressing the active chimeric sZPrC-TagRFP-ER (B, red) exhibit normal reticulate ER localization of the membrane-bound protease in the cytoplasm. Cells containing both the HsEg5 biosensor (C, violet) and sZPrC-TagRFP-ER protease exhibit cleavage activation of far-red fluorescence from the biosensor. Asterisk in panel A marks a cell that exhibits no reporter activation and expresses little or no sZPrC-TagRFP-ER. In contrast, cells co-expressing the HsEg5 biosensor (D, green) and inactive S135A-sZPrC-TagRFP-ER protease (E, red) do not exhibit detectable far-red fluorescence from the reporter (F, violet-background signal enhanced; no biosensor signal is detected). Scale bar = 25 μm.

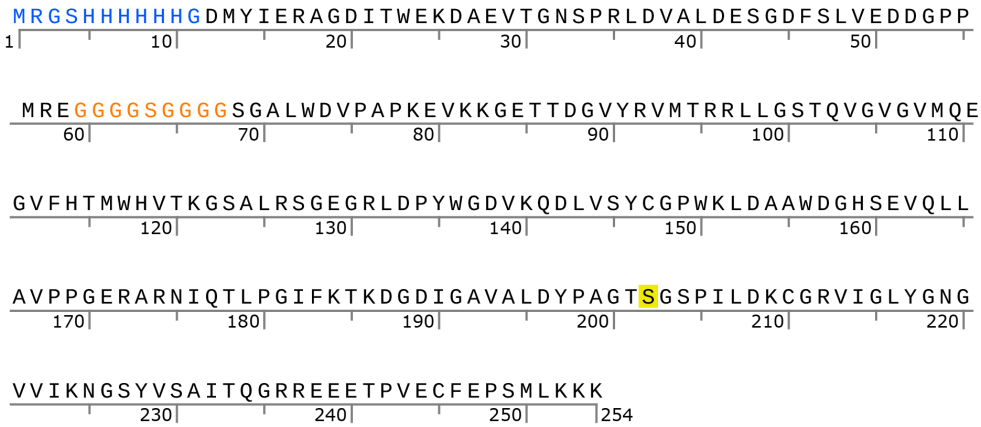

Figure S4. Protein sequence of the soluble chimeric Zika protease, related to Figure 1 and 3. 6xHis tag for protein purification is marked in blue, and a linker/loop connecting the NS2b segment to the NS3 peptidase domain is marked orange. The catalytic serine (S135) that is mutated to alanine in this and other constructs is highlighted yellow.

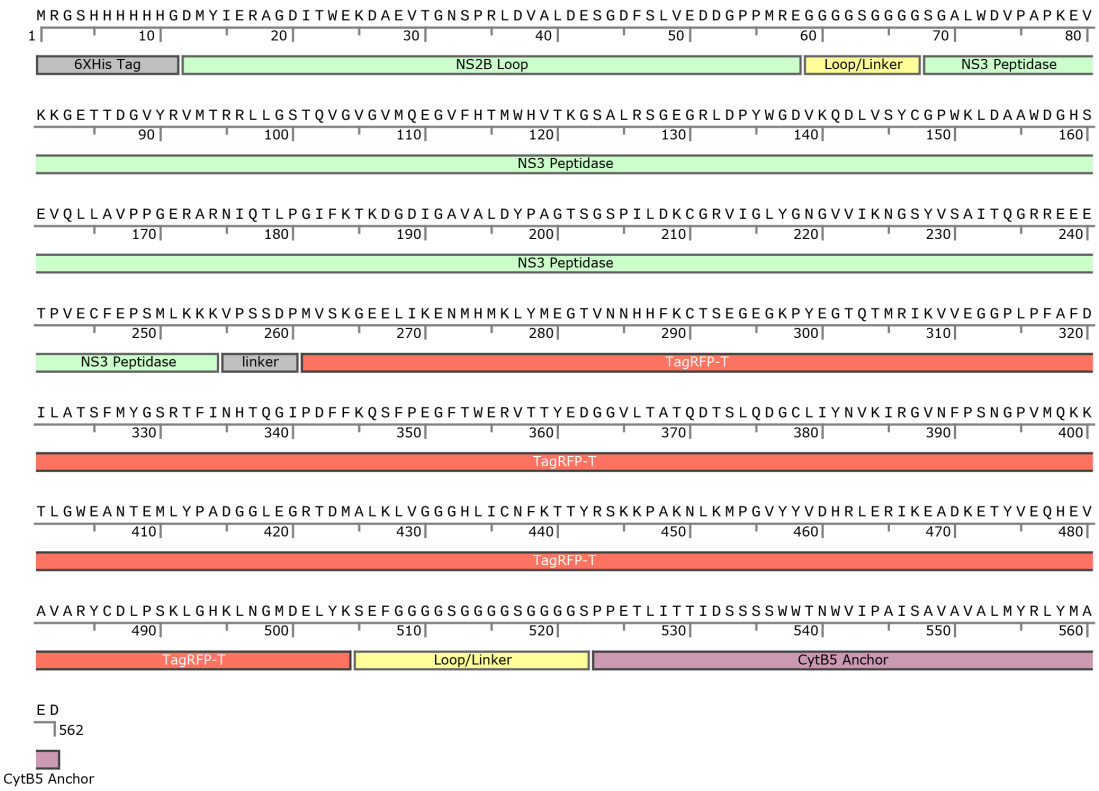

Figure S5. Protein sequence of Zika protease NS2b-NS3 chimera and integral ER membrane protein, related to Figure 5. The C-terminus of NS2b-NS3 chimera was fused with TagRFP-T. A transmembrane helix and ER-retention signal from cytochrome b5 reductase was added to the C-terminal of TagRFP-T. This overall chimera is resident in the ER outer membrane and mimics the behavior of the native protease.

Figure S6. Design and sequence of the native NS2b-NS3 Zika protease, related to Figures 5-8. This Zika sequence segment (violet) is shown in the context of the Zika polyprotein in Figure 4. Driven by the CMV promoter of pcDNA3.1, the native segment of the complete NS2b and NS3 peptidase domain is fused at the C-terminus to eGFP (green). This construct is expressed in the correct topology in the outer membrane of the ER. We do not detect this protein in mitochondria or other compartments (not shown).

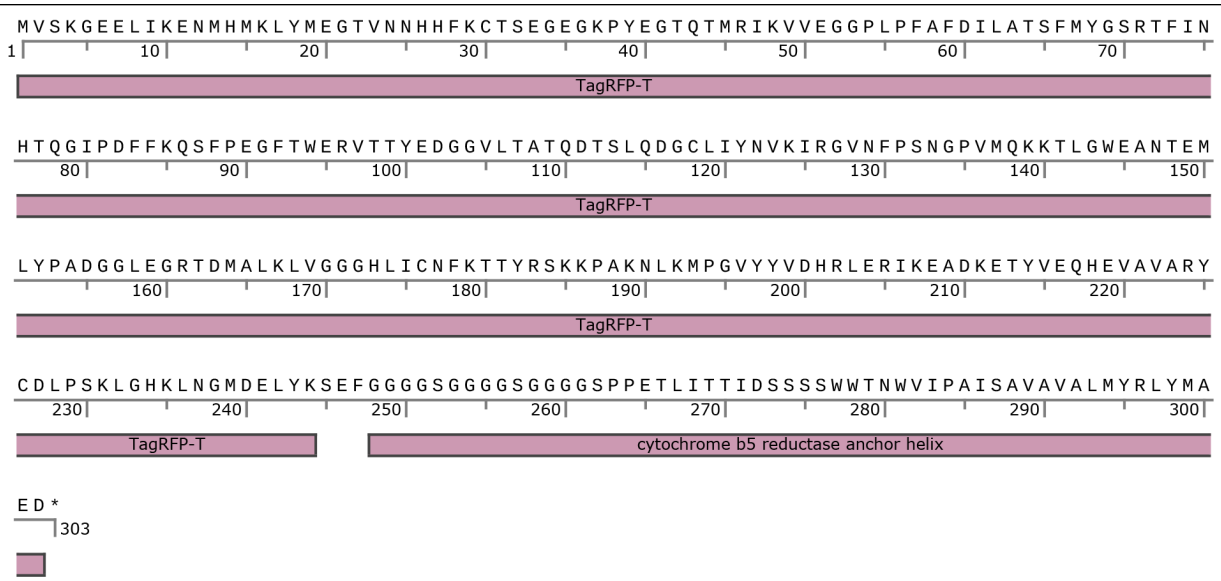

Figure S7. Design and sequence of TagRFP-b5 ^{anchor}, related to Figure 5. TagRFP-T was modified to include a C-terminal fusion to the cytochrome b5 reductase ER-anchoring helix. Complete with ER-retention signal, this construct was used to confirm ER localization of our Zika protease constructs.

Figure S8. Design and sequence of the HsEg5 biosensor reporter, related to Figures 8 and 9. The biosensor is based on bacterial infrared fluorescent phytochrome protein (IFP, Figure 8) that was originally designed to detect Caspase-3 activity *in vitro* (To et al., 2015). Inactive IFP is blocked from forming its chromophore by an exposed peptide loop; the original caspase target loop has been replaced with loop-8 of HsEg5 (DPRNKRG, Figure 8). The split-GFP components permit the GAF and PAS domains to remain associated (and to fluoresce) after the loop-8 segment is cleaved.

Transparent Methods

Soluble recombinant NS2BNS3 protease sequence, expression and purification.

We generated a soluble chimeric Zika protease (s-ZPrC) from a DNA construct corresponding to the NS2B-NS3–coding region of the Brazilian ZIKV isolate Paraiba_01/2015 strain (Topgene, Genbank: KX280026). We based the design of this chimera on earlier work on the Dengue homolog (Leung et al., 2001). Our construct is similar, but not identical, to other published soluble Zika protease constructs (Lei et al., 2016). Our synthetic construct codes for residues 50 to 96 of ZIKV NS2B, the C terminus of which is covalently linked via Gly_4-Ser-Gly_4 to the N terminus of NS3 (residues 1 to 187, Figure S4). The synthetic DNA of the NS2B-NS3 chimera with N-terminal 6XHis tag was inserted into pET21a (Thermo Fisher Scientific) to form s-ZPrC.

To generate the protease-inactive form of the soluble Zika protease (S135A-s-ZPrC), we mutated the active site Ser135 of the catalytic triad to Alanine in s-ZPrC using site-directed mutagenesis (Stratagene Quickchange) to generate S1235A-s-ZPrC.

Subsequently, the pET21A-NS2NS3 (s-ZPrC) and pET21A-S135A-NS2NS3 (S135A-s-ZPrC) expression vectors were transformed into the BL21 (DE3)-star strain of *E. coli* (Thermo Fisher Scientific). Cultures were grown in LB medium with ampicillin (100mg/L, FisherBiotech) at 37 ℃ until OD600 reached 0.8. The incubation temperature was reduced to 28 ℃ and protein expression was induced with 0.7mM IPTG (Goldbio). Cells were harvested 4 hours post-induction and cells were pelleted by centrifugation. The cell pellets were resuspended in lysis buffer containing 50mM Tris (pH8.0), 300mM NaCl, 25mM imidazole, 1mM PMSF, 0.04mg/ml DNAase I, 0.6mg/ml lysozyme and 5% glycerol. The resuspended cells were lysed at 4 ℃ using an Emulsiflex-05 Homogenizer (Avestin). The resulting lysates were centrifuged at 30,000g for 45min at 4 ℃ to remove cellular debris. The supernatant was filtered through a 0.22μm filter and loaded onto a HisTrap HP nickel column (GE Healthcare). The HisTrap columns were washed with 10 column volumes wash buffer (50mM Tris (pH8.0), 300mM NaCl, 25mM imidazole and 5% glycerol). The target proteins were eluted with a buffer containing 50mM Tris (pH 8.0), 300mM NaCl, 500mM imidazole and 5% glycerol using a linear imidazole gradient (25-500mM). To remove residual imidazole, the eluted target protein fractions were subsequently dialyzed overnight with buffer containing 50mM Tris (pH 8.0), 300mM NaCl, and 5% glycerol. Protein samples were then concentrated using centrifugal filtration (Centriprep 10kDA NMWL, Millipore) and stored at -80 ℃

Determination of enzyme kinetics of s-ZPrC with native and HsEg5 hexapeptides.

The kinetic parameters of s-ZPrC were determined essentially as described (Leung et al., 2001) using hexapeptides corresponding to P6-P1, which were labeled at their P1 position with chromogenic para-nitroaniline (pNA). Two of the labeled hexapeptides (PEPTIDE 2.0) were based on native Zika protease cleavage targets from within the viral polyprotein; Ac-FAAGKR-pNA (NS3/NS4A junction), and AcGLVKRR-pNA (NS4B/NS5 junction). A third hexapeptide was based on the identified cleavage site within HsEg5 loop8, Ac-DPRNKR-pNA (below). The lyophilized peptides were resuspended in ddH_2O to 20 mg/ml, aliquoted and stored at -80 ℃ until use. The enzyme activity assays were carried out at 28 ℃ in buffer containing 100mM Tris (pH9.0), 20% glycerol and 1mM 3-[(3-cholamidopropyl)-dimethylammonio]-1-propanesulfonnate (CHAPS), 100nM NS2BNS3 or NS2BNS3-S135A protease, and substrate hexapeptide from 0-4mM. The reaction contained 100nM NS2BNS3 or NS2BNS3-S135A protease and substrate peptide from 0-4mM. 100 μl reactions for each condition were assayed in 96 well plates and the release of pNA was monitored at 405 nm using a Spectromax M2 (Molecular Devices). Absorbance units were converted to the concentration of pNA released using a standard curve with free pNA (Sigma). The resulting data were analyzed using Michaelis-Menten kinetics using Prism (Graphpad) and illustrated using Igor Pro (Wavemetrics).

Identification of the primary s-ZPrC cleavage site within the HsEg5 motor domain.

The recombinant HsEg5 motor domain (residues 1-370) was expressed in BL21 (DE3) E. coli (Thermo Fisher Scientific) and purified by cation exchange chromatography as described (Wojcik et al., 2004). To identify any s-ZPrC cleavage sites within the HsEg5 motor domain, enzyme digests were carried out with HsEg5 motor domain and analyzed by SDS-PAGE. Peptide bands corresponding to HsEg5 cleavage products were excised and processed for LC-MS sequence identification. The enzyme digestion assays were carried out in in 50 µl reactions containing 10 µg purified s-ZPrC or S135A-s-ZPrC and 10 µg purified HsEg5 motor domain in a buffer containing 100mM Tris (pH9.0), 20% glycerol, 1mM CHAPS at 28 ℃ and incubated for 16 hours.

Reaction products were analyzed by SDS-PAGE using 4-12% Bis-Tris gradient gels (Thermo Fisher Scientific) followed by staining with Coomassie Blue (Sigma). Gels were imaged using Amersham Imager 600 (Amersham) and analyzed using gel tools in ImageJ (Schneider et al., 2012; Schindelin et al., 2012).

Selected peptide bands were cut from the gels and sequences determined by LC-MS. First, gel slices were destained by multiple additions of 50% Methanol and 50mm Ammonium Bicarbonate. Following destaining, the gel slices were dried to completion and 20 µl of 20 µg/ml trypsin was added and allowed to incubate overnight at 37 ℃. The next day, tryptic peptides were lyophilized (Speed Vac) and then resuspended in 20 µl of 2% ACN and 0.1% formic acid for LC-MS.

Subsequently, the samples were processed by a Dionex U3000 nano flow system coupled to a Thermo Orbitrap Fusion Tribrid Mass Spectrometer according to the manufacturer's standard protocols and procedures. Electrospray was achieved at 1.9kV. MS1 scans were performed in the Orbitrap utilizing a resolution of 240,000. Data-dependent MS2 scans were performed in the Orbitrap using High Energy Collision Dissociation (HCD) of 30% using a resolution of 30,000.

Finally, data analysis was performed using Proteome Discoverer 2.3 using SEQUEST HT scoring. Static modification included dynamic modification of oxidation of methionine (=15.9949). Parent ion tolerance was 10ppm, fragment mass tolerance was 0.02Da, and the maximum number of missed cleavages was set to 2. Only high scoring peptides were considered utilizing a false discovery rate (FDR) of 1%.

ER-resident Zika protease constructs and live-cell imaging.

We built two basic transfection constructs for the expression of ER-localized Zika protease. First, we added both a TagRFP-T fluorescent protein and ER transmembrane anchor to the C-terminus of the soluble ZPrC protein (s-ZPrC) sequence to result in s-ZPrC-TagRFP-ER (Figure S5). The ER transmembrane anchor **α**-helix was copied from the well-characterized ER-resident protein, cytochrome b5 reductase (Elahian et al., 2014; Ito and Sato, 1968). The soluble NS2B-NS3 ORF cassette was excised from pET21A-NS2NS3 (above) using PCR and cloned into TagRFP-T-pcDNA3.1 HindIII / KpnI sites resulting in C-terminal TagRFP. The resulting vector was linearized with EcoRI and EcoRV and synthetic DNA (Genscript) encoding a 17aa linker segment plus the complete cytochrome b5 reductase transmembrane ER signal peptide and retention domain (EFGGGGSGGGGSGGGGSPPETLITTIDSSSSWWTNWVIPAISAVAVALMY-RLYMAED) was added to complete the transfection construct.

Second, we built a more native version of the NS2B-NS3 protease that is comprised of an unmodified segment of the viral polyprotein with C-terminal eGFP moiety, n-ZPrC-eGFP (Figure S6). A segment including 4,225-5,171 bp of the Zika genome (GenBank, KX280026) spanning the complete NS2B and peptidase domain of NS3 (Ser1,373 – Lys1,687) was synthesized (Genscript) with EcoRV and NotI linkers to facilitate cloning into pcDNA3.1+C-eGFP (Addgene) at EcoRV/NotI polylinker sites to generate n-ZPrC-eGFP. To create S135A-n-ZPrC-eGFP, n-ZPrC-eGFP was subjected to site-directed mutagenesis to

change S135 of the peptidase catalytic triad to Ala (Quickchange, Stratagene). To create n-ZPrC-RFP670, the eGFP cassette of n-ZPrC was excised by NotI and XbaI digestion and replaced with the ORF of RFP670. RFP670 for this cloning step was PCR-amplified from pmiRFP670-N1 (Addgene #79987) with NotI and XbaI compatible overhangs. To create S135A-n-ZPrC-RFP670, the latter plasmid was subjected to site-directed mutagenesis to change S135 of the catalytic triad to Ala.

To label the ER membrane in cells, we tagged mScarlet with a C-terminal ER signal peptide and retention domain from cytochrome b5 reductase (above) in pcDNA3.1 (mScarlet-B5^{anchor}). We also utilized pCytERM-mScarlet N1 (Addgene #85066) to specifically label the ER membrane. pCytERM-mScarlet expresses the mScarlet fluorescent protein that is modified with an N-terminal type I ER membrane signal peptide & anchor derived from cytochrome p450.

The final sequences of all assembled constructs were confirmed by sequencing. CDNA and chromosomes were visualized in live cells by transfection of mScarlet-H2A C1 histone (Addgene #85051).

To engineer the HsEg5 biosensor reporter of Zika protease activity, we modified a construct originally designed to report tobacco etch virus protease (TEV) activity, pcDNA3.1-iTEV (Addgene #64276). This construct utilizes a split-GFP to organize a circularly permutated monomeric infrared fluorescent protein. The infrared fluorescent protein is kept in a misfolded condition by a peptide loop that contains a TEV protease cleavage site. Therefore, to modify the construct to detect Zika protease activity, pcDNA3.1-iTEV was digested with AfeI and EcoRI to excise the 69 bp containing the TEV cleavage site, and subsequently this segment was then replaced with the following 65 bp sequence that instead contains the DPRNKRG HsEg5 loop8 site;
GCTGGCGGAAACTTGTGCGAACCGCATCGCGACGCTGGAGAGCGATCCCCG-TAACAAGAGAGGAG.
The 3' end of the cloned 65 bp dbl-stranded fragment contains an EcoRI overhang.

All transfection plasmids were transfected into various cell lines, including HEK293-T, HeLa, and MCF-7, using the calcium phosphate transfection method (Invitrogen), or using Lipofectamine 3000 (ThermoFisher), following the manufacturer's protocols. Cells were plated onto heated glass-bottom 35mm culture dishes (Delta-T, Bioptechs) treated with Cell-Tak (Corning) and allowed to recover for 24 hrs. after transfection before imaging. Cells were recorded in timelapse 24-48 hr. after transfection. Live-cell confocal imaging was performed on a Zeiss Axiovert 200 equipped with a Yokogawa spinning disk confocal and Andor 3-channel solid-state laser combiner. Cells were maintained under CO_2 and at 37 ℃ using both a plate warmer and objective warmer (Bioptechs). To calculate the metaphase:anaphase ratios, HEK293-T cells were co-transfected with mScarlet-H2A C1 (Addgene #85051) and n-ZPrC-eGFP or s-ZPrC-eGFP and scored after 24 hrs. Data was compiled from three separate transfection experiments of three plates separately for each tested construct. An average of 100 mitotic cells per dish were counted to calculate the M/A ratio. Reported values are ± S.D.

The confocal workstation components were controlled by ImageJ together with the micromanager plugin (Edelstein et al., 2010). Images were captured with a Hamamatsu Orca-ER and processed with ImageJ and Affinity photo (Serif) for publication. Long-term timelapse images were converted to movies using Quicktime (Apple Computer) and Handbrake (https://handbrake.fr/). The graphical abstract, Figure 8, and Figure 10 were created with BioRender.com.

Supplemental References

Edelstein, A., Amodaj, N., Hoover, K., Vale, R., and Stuurman, N. (2010). Computer control of microscopes using μManager. Curr Protoc Mol Biol, *Chapter 14*, Unit14.20. 10.1002/0471142727.mb1420s92.

Elahian, F., Sepehrizadeh, Z., Moghimi, B., and Mirzaei, S.A. (2014). Human cytochrome b5 reductase: structure, function, and potential applications. Crit Rev Biotechnol, *34*, 134–143. 10.3109/07388551.2012.732031.

Ito, A., and Sato, R. (1968). Purification by means of detergents and properties of cytochrome b5 from liver microsomes. Journal of Biological Chemistry, *243*, 4922–4923. https://doi.org/10.1016/S0021-9258(18)93204-7.

Lei, J., Hansen, G., Nitsche, C., Klein, C.D., Zhang, L., and Hilgenfeld, R. (2016). Crystal structure of Zika virus NS2B-NS3 protease in complex with a boronate inhibitor. Science, *353*, 503–505. 10.1126/science.aag2419.

Leung, D., Schroder, K., White, H., Fang, N.X., Stoermer, M.J., Abbenante, G., Martin, J.L., Young, P.R., and Fairlie, D.P. (2001). Activity of recombinant dengue 2 virus NS3 protease in the presence of a truncated NS2B co-factor, small peptide substrates, and inhibitors. J Biol Chem, *276*, 45762–45771. 10.1074/jbc.M107360200.

Schindelin, J., Arganda-Carreras, I., Frise, E., Kaynig, V., Longair, M., Pietzsch, T., Preibisch, S., Rueden, C., Saalfeld, S., Schmid, B. et al. (2012). Fiji: an open-source platform for biological-image analysis. Nat Methods, *9*, 676–682. 10.1038/nmeth.2019.

Schneider, C.A., Rasband, W.S., and Eliceiri, K.W. (2012). NIH Image to ImageJ: 25 years of image analysis. Nat Methods, *9*, 671–675. 10.1038/nmeth.2089.

Wojcik, E.J., Dalrymple, N.A., Alford, S.R., Walker, R.A., and Kim, S. (2004). Disparity in allosteric interactions of monastrol with Eg5 in the presence of ADP and ATP: a difference FT-IR investigation. Biochemistry, *43*, 9939–9949. 10.1021/bi048982y.